ARMY RESEARCH LABORATORY

Structural Analysis of Reinforced "SICPS" Shelter Floor Panel Subjected To Rail Impact Loading

Paul Cavallaro

ARL-TR-514

October 1994

REPORT DOCUMENTATION PAGE

Form Approved
OMB No. 0704-0188

1. AGENCY USE ONLY *(Leave blank)*

2. REPORT DATE
October 1994

3. REPORT TYPE AND DATES COVERED

4. TITLE AND SUBTITLE
Structural Analysis of Reinforced "SICPS" Shelter Floor Panel Subjected to Rail Impact Loading

5. FUNDING NUMBERS

6. AUTHOR(S)
Paul V. Cavallaro

7. PERFORMING ORGANIZATION NAME(S) AND ADDRESS(ES)
U.S. Army Research Laboratory
Watertown, MA 02172-0001
ATTN: AMSRL-MA-PC

8. PERFORMING ORGANIZATION REPORT NUMBER
ARL-TR-514

9. SPONSORING/MONITORING AGENCY NAME(S) AND ADDRESS(ES)
U.S. Army Natick Research, Development & Engineering Center
Natick, MA 01760-5010

10. SPONSORING/MONITORING AGENCY REPORT NUMBER

19941205 107

11. SUPPLEMENTARY NOTES

12a. DISTRIBUTION/AVAILABILITY STATEMENT
Approved for public release; distribution unlimited.

12b. DISTRIBUTION CODE

13. ABSTRACT *(Maximum 200 words)*

ABSTRACT

Structural analyses related to a Standardized Integrated Command Post Shelter (SICPS) mounted to a High Mobility Multi-Purpose Wheeled Vehicle (HMMWV) were conducted to determine the response of the former to rail impact loading conditions (shown in Figure 1). The Finite Element Method (FEM) was used to establish the relative structural contributions of the floor panel components when subjected to simulated rail impact. Stress fields of the floor panel face sheets were obtained and compared for reinforced and non-reinforced (baseline) models subjected to static body forces. Conclusions regarding the structural performance of the floor reinforcements were made based on these comparisons.

14. SUBJECT TERMS
Finite element analysis, Finite element modelling, Shelters, Composite sandwich panels, Rail impact

15. NUMBER OF PAGES
35

16. PRICE CODE

17. SECURITY CLASSIFICATION OF REPORT	18. SECURITY CLASSIFICATION OF THIS PAGE	19. SECURITY CLASSIFICATION OF ABSTRACT	20. LIMITATION OF ABSTRACT
Unclassified	Unclassified	Unclassified	UL

NSN 7540-01-280-5500

Standard Form 298 (Rev. 2-89)
Prescribed by ANSI Std. Z39-18
298-102

CONTENTS

PAGE

INTRODUCTION.. 1

MODEL DEVELOPMENT & DESCRIPTION................................. 2

RESULTS... 8

CONCLUSIONS... 12

RECOMMENDATIONS... 13

ACKNOWLEDGEMENTS.. 13

APPENDIX

SICPS Mounted HMMWV in Rail Transport Configuration.......... 14

Floor Drawings... 15-20

Finite Element Model of Floor & Reinforcements.............. 21

Displaced Models... 22-24

Displacement Contour Plots................................. 25-27

Face Sheet Stress Contour Plots............................ 28-33

INTRODUCTION

The SICPS floor, shown in Figures (2,3), was a sandwich panel constructed of 0.125" thick 6061-T6 aluminum face sheets bonded to a 1.210" thick paper honeycomb core. Two mechanical fastening methods for securing the SICPS floor to the cargo area of the HMMWV were developed. The first method employed two transverse integral stiffeners and two sets of face sheet mounted doubler plates as shown in Figure (4). The second method consisted of forward and rear external mounting brackets and was selected for subsequent SICPS production. The latter bracket is shown in the inset view of Figure (1). However, the transverse stiffener/doubler plate assemblies, while no longer serving as the tie down means, continued to be manufactured and installed in current production runs. The goals of this effort were to: (1) determine if the transverse beams with or without the doubler plates had any significant contribution to the structural integrity of the shelter while no longer serving as a tie down means and (2) develop Finite Element Models (FEM's) of the floor panel which could subsequently be expanded into complete SICPS shelter models. If no beneficial influence was provided by these reinforcements, they would be eliminated from the design to achieve reductions in weight and both material and labor costs.

The stiffeners were 6061-T6 aluminum box beams with outer dimensions of 2.000" width by 1.090" height with a 0.060" uniform wall thickness. Adjacent core sections were bonded to the outer web surfaces of the transverse beams using film adhesive. Close-out extrusions (not shown) sealed the outer edges of the floor panel and allowed for attachment of the wall sections to the floor. However, the transverse beams were allowed to "float", that is, their

ends were not attached to the close-out members. It was expected that the structural contributions of the transverse beams were not maximized since the beams could not directly transfer loads to the close-out members and side walls. The face sheets were then bonded entirely over the core and beam surfaces to complete the floor panel construction. Two sets of doubler plates made of 0.150" thick 6061-T6 aluminum were mechanically fastened to the lower face sheet of the floor panel in the wheel well regions as shown in Figures (2, 5-7).

MODEL DEVELOPMENT & DESCRIPTION

The structural analyses discussed herein were conducted using the NISA-II finite element software[1] and were limited to linearly elastic, static formulations. Only the SICPS floor panel could be sufficiently modeled due to limitations on the maximum number of Degrees of Freedom (DOF's) available. In light of this limitation and the absence of a dynamic formulation, the approach developed was expected to provide reasonable solutions for evaluating the relative structural effectiveness of the reinforcements investigated.

Due to symmetry in geometry, material properties, loading and boundary conditions of the SICPS floor, only one half of the floor panel was modeled as shown in Figure (8). Four possible combinations of the existing reinforcements were modeled. These consisted of: (1) transverse beams and doubler plates, (2) no transverse beams and no doubler plates, (3) transverse

1. NISA-II, Version 92.0, Engineering Mechanics Research Corporation, Troy Michigan

beams only, and (4) doubler plates only.

Instrumented rail impact tests of fully loaded HMMWV mounted SICPS Shelters were conducted by the U.S. Army Natick Research, Development and Engineering Center (NRDEC) at the Combat System Testing Agency (CSTA) in Aberdeen Proving Grounds, Maryland. Testing revealed that peak reactions at the forward mounting kit totalled 25 kips (25,000 lbs.) in the direction opposite impact. Therefore, a total reaction constraint of 25 kips for the forward mounting kit was imposed in each of the models. This constraint was satisfied by applying initial static body forces in the plane of the floor (X-Y plane) so as to represent inertial loading. Next, the ratio of the sum of the four forward mounting kit fastener reactions to the applied body force was computed for each model. Finally, adjusting the body force according to this ratio, the model was re-run to obtain the solution that satisfied the 25 kip reaction constraint. Body forces used to represent the inertial loads were mutually reacted by the fasteners within both mounting kits. Since the body forces were mass dependent and only the SICPS floor was considered, the accelerations used to generate the body forces in the floor models have no correlation whatsoever to those imposed on the actual shelter during rail impact.

Each model included the exact tie down fastener locations in both the front and rear mounting kit regions of the floor panel. The fasteners were represented as elastic offsets using 1.00" diameter steel beam elements with fixed end nodes (refer to Figure 8). Offset lengths were determined as the unsupported or free span lengths of the fasteners measured from the floor panel middle surface to the receiving bracket attached to the HMMWV. These lengths were 4.22" and 1.88" for the forward and rear mounting kits respectively.

The floor panel was modeled using NISA type 33 laminated sandwich elements and type 39 3-D general beam elements. Orders of the isoparametric functions were quadratic and linear for the sandwich and beam elements respectively. Geometric properties of the transverse members were determined and shown in Table (1). Since the doubler plates did not cover the entire surface of the bottom face sheet, two sets of sandwich elements were required to model the floor. The only difference between the sets of sandwich elements was that elements located in the regions defining the doubler plates had thicker lower ace sheets. This thickness was equal to the sum of the lower face sheet and doubler plate thickness. The lamination sequences for all sandwich elements used are defined in Table (2).

A total of five layers was used to develop the sandwich elements although only three physically distinct layers (adhesive layers excluded) actually existed. The NISA-II program provided stress resultant output only at the middle surface of each layer. In order to obtain the maximum flexure stress at the outer surfaces of the sandwich elements, it was necessary to define significantly thin layers (0.001" thick) within the aluminum layers. By doing so, stress resultants near the outer surfaces of the face sheets were approximated as being equivalent to those located 0.0005" in from the outer surfaces. Material properties required by the models for the aluminum and honeycomb layers are presented in Table (3). The aluminum face sheets, doubler plates and transverse box beams were modeled as an isotropic material while the honeycomb core was modeled as an orthotropic medium. Due to the manufacturing process used to produce honeycomb, properties in the longitudinal (parallel to the ribbon) direction were different from those in

Table 1 - Transverse Beam Section Properties

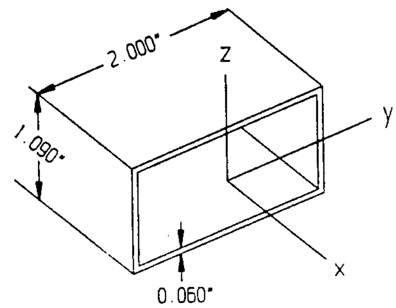

A = cross sectional area = 0.3564 in^2

I_{yy} = moment of inertia about y-y (horizontal) axis = 0.0729 in^4

I_{zz} = moment of inertia about z-z (vertical) axis = 0.1896 in^4

J = polar moment of inertia = $I_{yy} + I_{zz}$ = 0.2625 in^4

(xyz) = local coordinate system for beam elements

Table 2 - Lamination Sequence for Sandwich Elements

Doubler Reinforced Sandwich Elements

Layer	Thickness	Angle	Material
1	0.001	0	Aluminum
2	0.024	0	Aluminum
3	1.210	0	Honeycomb
4	0.149	0	Aluminum
5	0.001	0	Aluminum

Total Element Thickness: 1.385"

Non-Reinforced Sandwich Elements

Layer	Thickness	Angle	Material
1	0.001	0	Aluminum
2	0.024	0	Aluminum
3	1.210	0	Honeycomb
4	0.024	0	Aluminum
5	0.001	0	Aluminum

Total Element Thickness: 1.260"

the transverse direction. Transverse shear deformation effects[2] of the core were included in the formulation of the sandwich elements used. The following mechanics of materials assumptions employed were that: (1) the face sheets were loaded in a state of plane stress (i.e.; no transverse or through-the-thickness normal stresses were developed), (2) the face sheets were relatively thin compared to the core, (3) the core supported the applied transverse shear stresses S_{xz} and S_{yz}, and (4) the bond layers between the face sheets and core layers were 'perfect' (i.e.; zero thickness with no deformation allowed). Hence, as shown in Table (3), zero transverse shear stiffnesses were assigned to the face sheets and a zero transverse normal stiffness was given to the core. Due to the lamination sequence used for the doubler region elements (i.e.; combined thicknesses of the lower face sheet and doubler plates), two conditions were enforced: (1) no doubler plate fasteners were modeled and (2) no relative slip was allowed between the lower face sheet and doubler plates.

The computational limits on model size allowed for only consideration of the floor panel. Therefore, the stiffening effects of other SICPS panels (i.e.; roof, wheel wells, side and end walls) on the floor could not be represented accurately. However, these effects could be bound by imposing exterior edge displacement conditions ranging from simple (or roller) supports to fixed (clamped) supports. The assumption of simple supports on the exterior edges of the floor was invoked for two purposes. First, clamped DOF's on the exterior edges would undesirably react the body force loading away from the mounting kits. Secondly, simple supports provided conservative results by restraining displacements in the Z direction while permitting the in-plane

2. JONES, R. M., Mechanics of Composite Materials, 1975, Hemisphere Publishing Corp., pp. 299-309.

Table 3 - Material Properties

Property	6061-T6 Aluminum	Paper Honeycomb
E_x, psi	10.0e+06	0
E_y, psi	10.0e+06	0
E_z, psi	10.0e+06	0
ν_{xy}	0.334	
ν_{xz}	0.334	
ν_{yz}	0.334	
G_{xy}, psi	3.748e+06	1.30e+04
G_{xz}, psi	0	7.00e+03
G_{yz}, psi	0	7.00e+03
Wgt Dens, #/in^3	0.098	1.45e-03

Table 4 - Model Matrix

Model Name	Load	Trans. Beams	Doublers	Offsets(in) Fwd/Rear	Ext. Edge B/C's	Model Wgt (#)	X-Accel (in/s^2)
Floor8	BF	X	X	4.22/1.82	No Z Disp.	27.86	-1780.00
Floor9	BF			4.22/1.82	No Z Disp.	17.29	-2570.56
Floor10	BF	X		4.22/1.82	No Z Disp.	19.60	-2294.78
Floor11	BF		X	4.22/1.82	No Z Disp.	25.56	-1929.22

(BF=BODY FORCE LOADING)

rotation vectors along the exterior edges to rotate freely. Boundary conditions assigned to DOF's located along the line of symmetry (the longitudinal or lengthwise centerline of the floor) were restrained as follows:

$$V = U' = W' = 0$$

<u>where</u>: V = displacement vector in the width (Y-axis) direction
U' = rotation vector in the longitudinal (X-axis) direction
W' = rotation vector in the normal (Z-axis) direction

(Refer to coordinate system shown in Fig. 8)

These restrained DOF's forced the half floor model to behave identically as the full floor model would under load. An additional restraint was that the sandwich elements have no normal rotational DOF's. The matrix shown in Table (4) depicts the loading and reinforcement combinations used in each analysis performed. The were no graphical differences between the four models which were displayed soley by Figure (8). The doubler plate and transverse beam elements, shown separately in Figure (8), directly superimposed on the floor panel elements.

RESULTS

Output for each model included deformed views of the floor panel elements and, where applicable, the doubler plates and transverse beams (see Figures 9-11). Middle (neutral) surface displacement components along the global X, Y, Z directions of the floor panel elements were plotted in Figures (12-14). Principal (or material direction) stresses S_{xx}, S_{yy} and S_{xy} for the upper and lower face sheet middle surfaces (layers 1 and 5) were plotted in Figures (15-

20). [Remaining consistent with NISA-II's designation of principal stresses obtained from its composite sandwich element, the reader may choose to substitute the conventional S_{11}, S_{22} and S_{12} designations respectively.] Only in-plane stresses were obtained for the face sheets due to the plane stress assumption used. Minimum and maximum values of the face sheet stresses were tabulated in Table (5) along with their designated locations. The relevant stress components for the core (layer 3) were the transverse shears S_{xz} and S_{yz}. However, the core stress components were essentially equal to zero and were not plotted. Displacement and stress component contour plots were conveniently arranged to allow for direct comparison of results between the four models considered.

A review of the stress component plots from models FLOOR9 and FLOOR10 (no reinforcements vs. transverse beams only) established the effectiveness of the transverse beams independently of the doubler plates. The FLOOR10 beam reinforced model revealed that a minimal (500 to 700 psi) reduction of local (transverse beam regions) S_{xx} stress was acheived in both face sheets when compared to the baseline panel of model FLOOR9. The unbalanced face sheet S_{xx} stresses shown in Table (5) indicated that bending was present within the floor. This was a direct result of the fact that the body force loads were eccentrically reacted by the elastic offsets (refer to the displaced model geometries shown in Figures 9-11). Reductions in local and far-field values of the S_{yy} and S_{xy} stress components were negligible for both face sheets.

Stress contours from models FLOOR8 and FLOOR11 (doublers only vs. doublersand transverse beams) indicated that no reinforcement coupling effects

Table 5 - Face Sheet Stresses (ksi)

FLOOR8 - DOUBLER PLATES & TRANSVERSE BEAMS

Face Sheet	S_{xx} (min/max) (loc/loc)	S_{yy} (min/max) (loc/loc)	S_{xy} (min/max) (loc/loc)
UPPER	46.56/29.85 A/B	-32.79/9.83 C/B	-11.10/19.89 D/E
LOWER	-57.54/28.48 A/B	-36.97/11.08 C/G	-16.22/26.04 D/E

FLOOR9 - NO DOUBLER PLATES & NO TRANSVERSE BEAMS

Face Sheet	S_{xx} (min/max) (loc/loc)	S_{yy} (min/max) (loc/loc)	S_{xy} (min/max) (loc/loc)
UPPER	-46.53/58.53 A/B	-35.14/13.32 C/H	-10.39/26.51 D/I
LOWER	-60.88/61.64 A/B	-39.59/13.30 C/H	-16.55/27.82 J/E

FLOOR10 - TRANSVERSE BEAMS & NO DOUBLER PLATES

Face Sheet	S_{xx} (min/max) (loc/loc)	S_{yy} (min/max) (loc/loc)	S_{xy} (min/max) (loc/loc)
UPPER	-46.42/59.56 A/B	-34.68/13.07 C/H	-10.53/26.35 D/I
LOWER	-60.70/62.71 A/B	-39.10/13.04 C/H	-16.55/27.54 J/E

FLOOR11 - DOUBLER PLATES & NO TRANSVERSE BEAMS

Face Sheet	S_{xx} (min/max) (loc/loc)	S_{yy} (min/max) (loc/loc)	S_{xy} (min/max) (loc/loc)
UPPER	-46.74/29.21 A/B	-33.00/9.72 C/H	-11.05/20.01 D/E
LOWER	-57.58/29.09 A/F	-37.20/10.59 C/G	-16.05/26.24 D/E

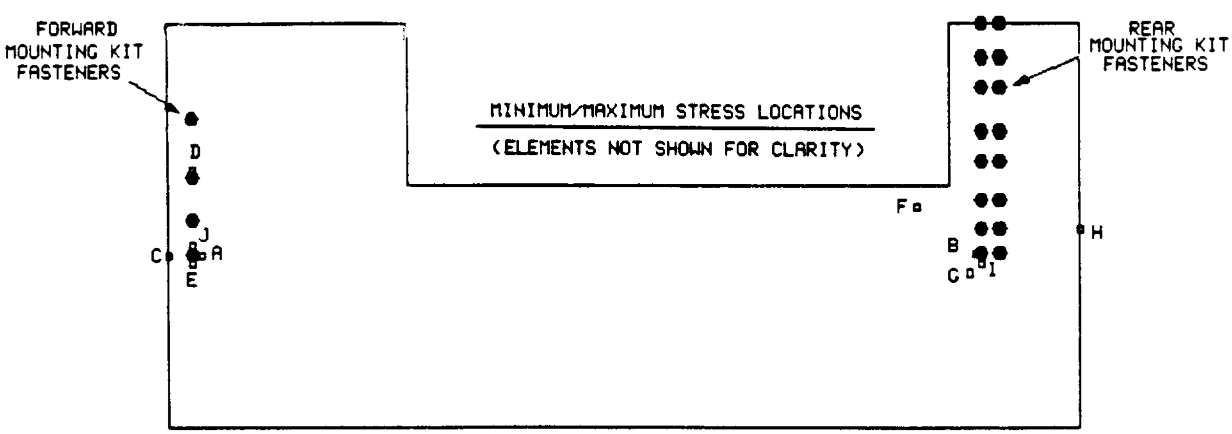

were provided by the transverse beams in the presence of the doubler plates. Negligible decreases of the upper face sheet Sxx stress (200 to 500 psi) were made in the local region of the forward transverse beam. However, a 600 psi increase of the upper face sheet S_{xx} stress developed in the vicinity of the rear transverse beam. The far-field upper face sheet S_{xx} stress increased due to the presence of the beams by approximately 500 psi. The lower face sheet S_{xx} stress at the forward transverse beam increased by 375 psi. The rear transverse beam provided a 510 psi decrease in the local S_{xx} stress of the lower face sheet. Far-field S_{xx} stress in the upper and lower face sheets decreased in the presence of the transverse beams by approximately 500 psi.

Comparisons between the doubler reinforced (FLOOR8, FLOOR11) and the non-doubler reinforced (FLOOR9, FLOOR10) models revealed a 50% reduction in the maximum face sheet tensile S_{xx} stress. In each model, the peak upper face sheet tensile S_{xx} stress occurred forward of the bottom left fastener of the rear mounting kit. However, the maximum lower face sheet tensile S_{xx} stresses in the doubler reinforced models were located away from the rear mounting kit (refer to Table 5). The effect of the rear mounting kit doubler plate was to redistribute the body force loading in a more uniform manner. The maximum compressive S_{xx} stresses for both face sheets occurred to the right of the lowest forward mounting kit fastener in all four models. The presence of the doubler plates on the lower face sheet induced a stiffness imbalance between the upper and lower face sheets. This imbalance caused further rotational deformation of the floor in addition to that from the eccentric reactions.

Significant reductions in the S_{xx} stresses of the upper and lower face sheets were achieved in both wheel well corners by the doubler plates.

Reductions for the upper and lower face sheets in the forward wheel well corner were 63% and 78% respectively. At the rear wheel well corner, the reductions were 55% and 61% for the upper and lower face sheets respectively. Similar reductions were observed in the S_{yy} and S_{xy} stresses of both face sheets at the wheel well corners.

Full extension of the transverse box beams to the simply supported floor edges was investigated in a separate model. Using in-plane body force loading, no significant reductions in face sheet stresses were realized. No improvements were made in transferring face sheet stresses to the beams.

The effects of increasing the tranvserse beam wall thickness were addressed with another model subjected to an in-plane body force. Here, the wall thickness was increased from 0.060" to 0.120" while the outer cross section dimensions of the beam were maintained. This increased the moments of inertia I_{yy} and I_{zz} by 173% and 160% respectively. No significant improvements were acheived in reducing the face sheet stresses.

CONCLUSIONS

The analytical models developed in this effort assessed the relative structural contributions of the SICPS floor components when subjected to simulated rail impact conditions using in-plane body forces. Stress distributions in both face sheets indicated that no significant reductions were acheived by the inclusion of the transverse box beams. Doubler plates used in conjunction with only the lower face sheet resulted in a stiffness imbalance with respect to the panel's middle surface. This induced further

rotational deformation of the floor in addition to that caused by the offset mounting kit fasteners. Both doubler plates substantially reduced the lower face sheet S_{xx} stress in the forward and rear wheel well corners by 55% and 78% respectively. The rear doubler plate assembly provided a 50% reduction of maximum tensile S_{xx} stress in the lower face sheet.

RECOMMENDATIONS

1. Eliminate the two transverse box beams from the SICPS shelter floor panel.
2. Optimize the sizes of the forward and rear doubler plate assemblies to achieve manufacturing cost and weight reductions.
3. Reduce peak compressive face sheet S_{xx} stresses at the forward mounting kit by using a suitably sized doubler plate.
4. Determine the minimum number of mechanical fasteners required in the rear mounting kit. Optimize fastener spacing to reduce local stress gradients in the face sheets.
5. Expand the floor finite element models into full SICPS shelter models. Conduct an absolute transient stress analysis of the complete SICPS shelter using force-time and acceleration-time data obtained from instrumented rail impact testing.

ACKNOWLEDGEMENTS

The author would like to express sincere appreciation to the staff of the Tactical Shelters Branch at the Natick Research, Development and Engineering Center. Special thanks are made to Mr. Arthur Murphy, Mr. Melvin Jee and Mr. James Cullinane for providing the technical expertise and necessary funding.

APPENDIX

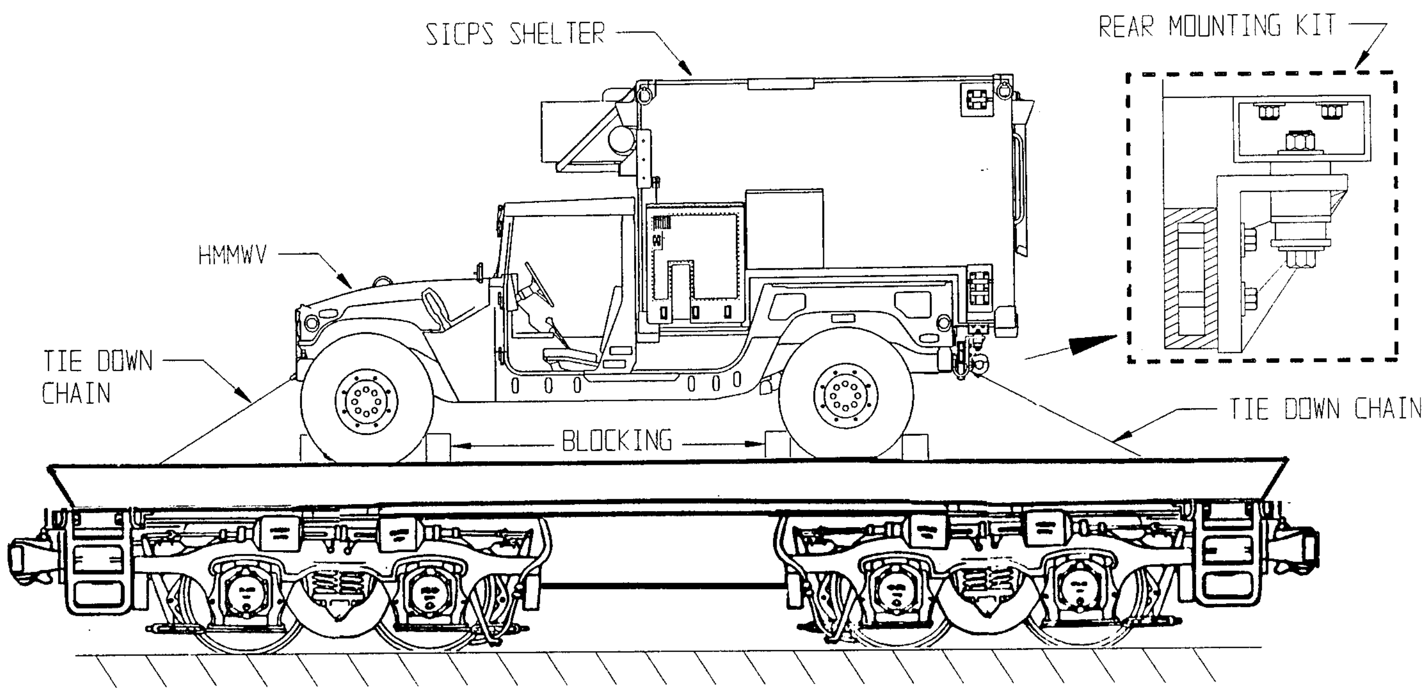

Fig. (1) SICPS w/ HMMW in Rail Transport Configuration

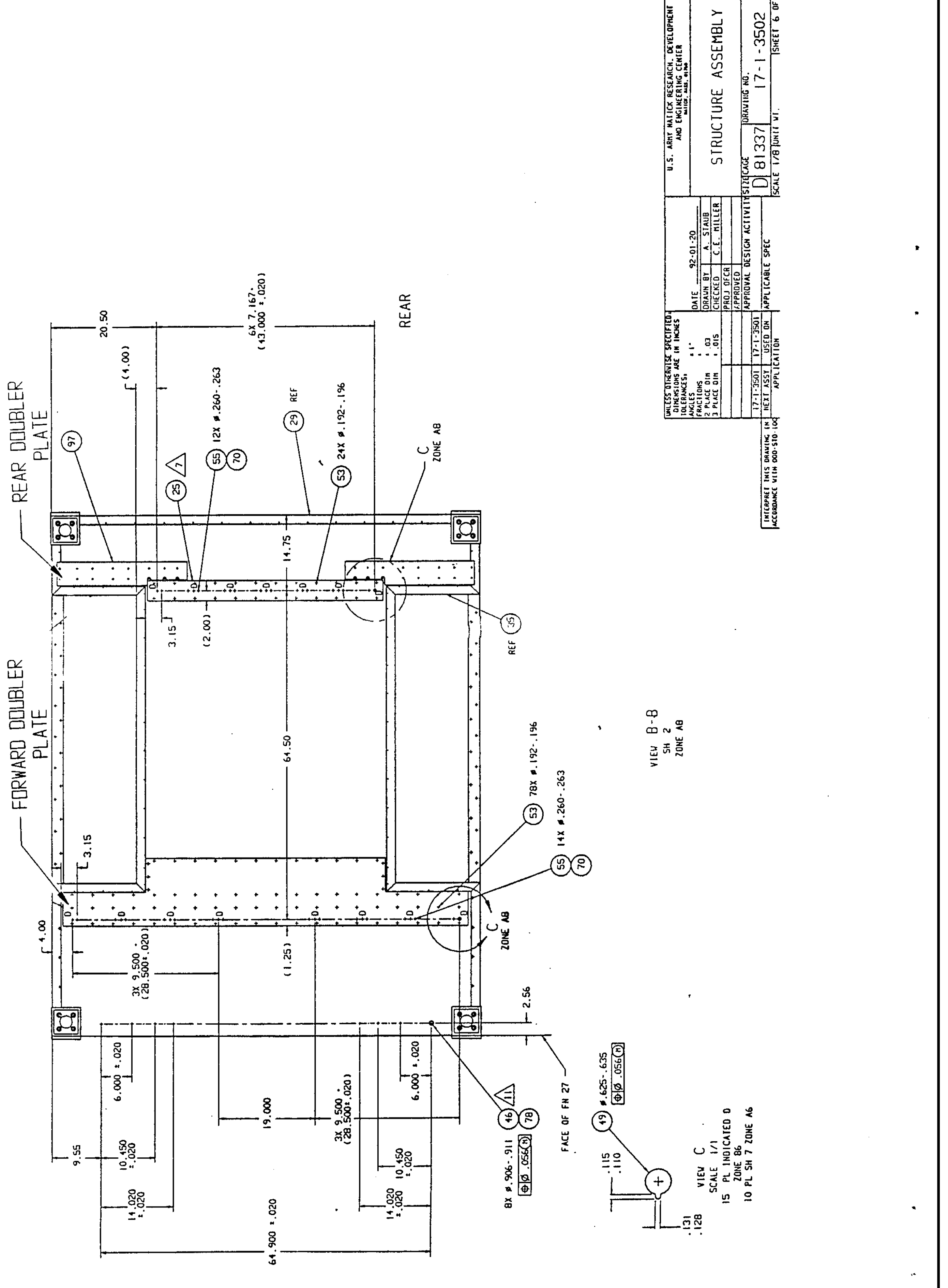

Fig. (2) SICPS Floor Panel w/ Doubler Plates Shown

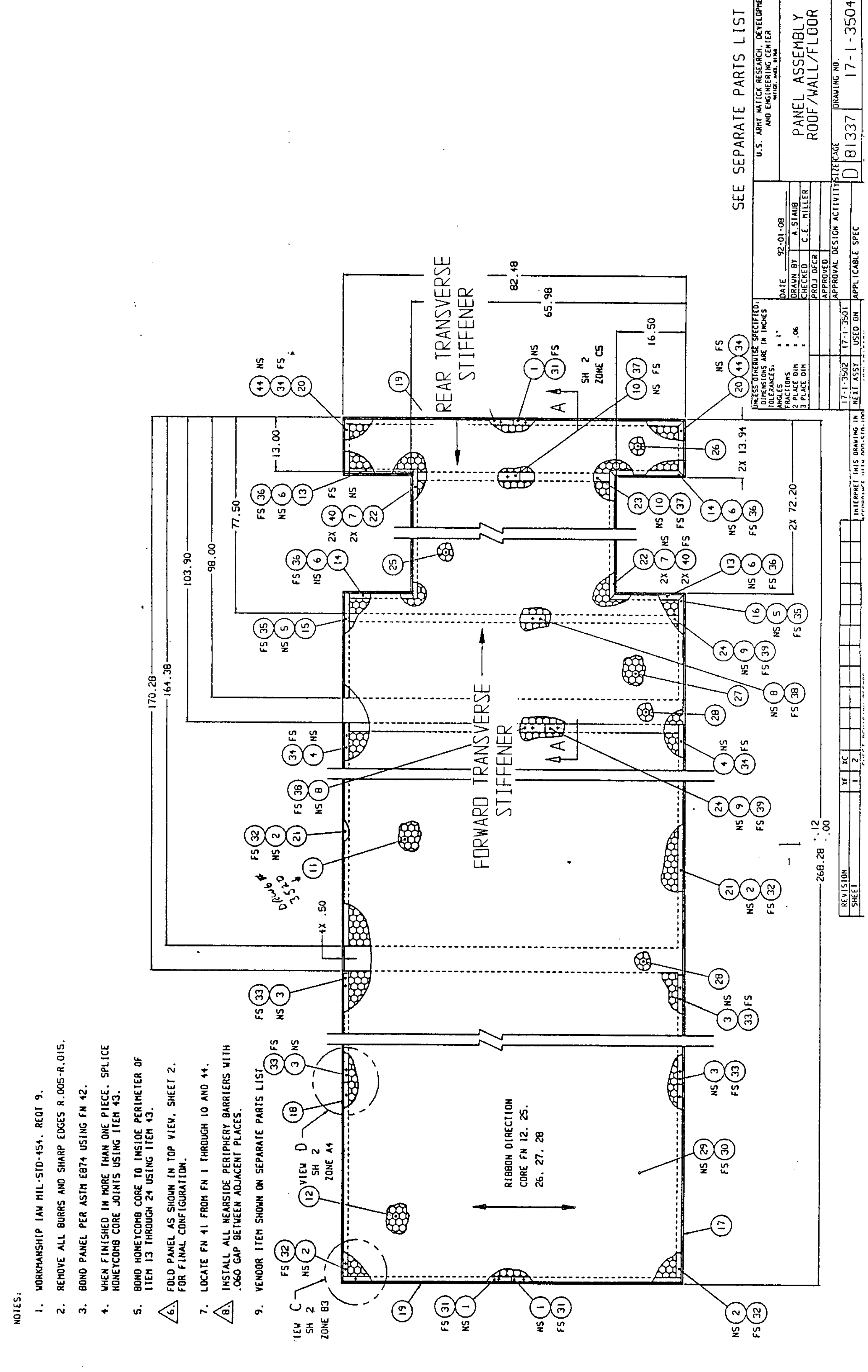

Fig. (3) SICPS Floor Panel w/ Transverse Box Beams Shown

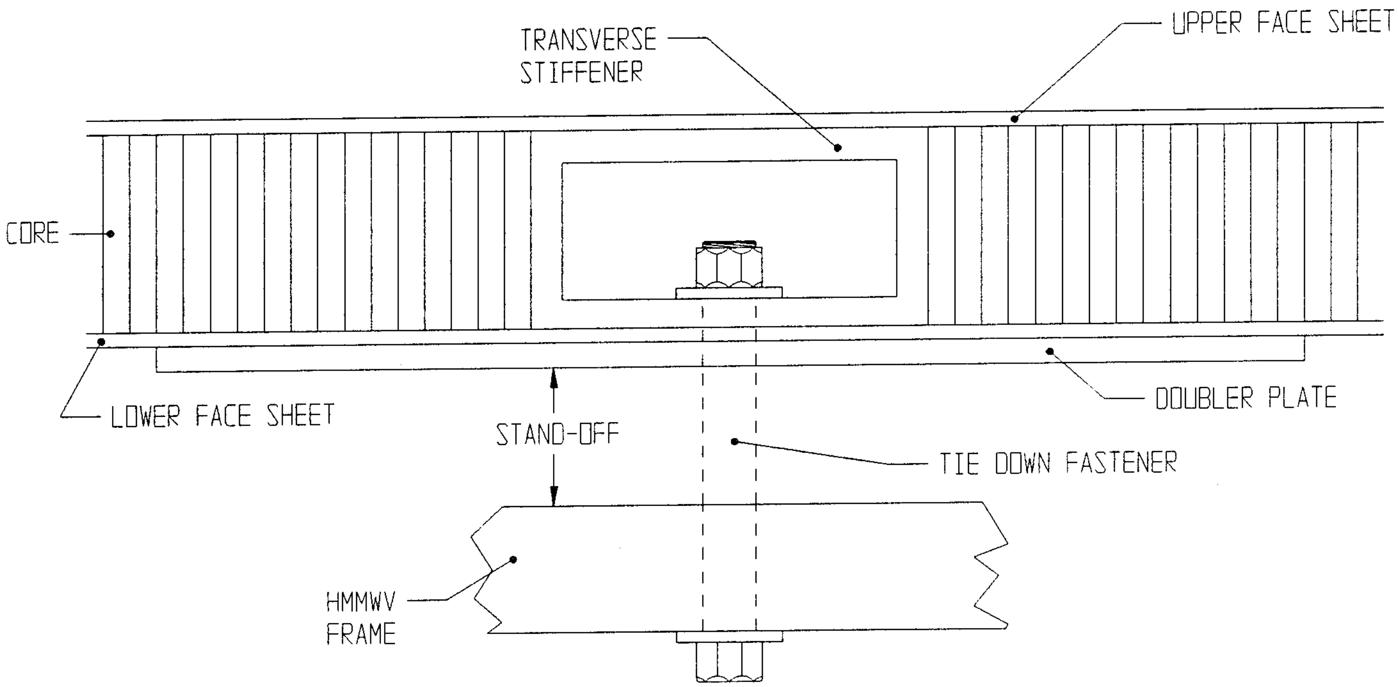

Fig. (4) Floor Panel w/ Integral Transverse Stiffener & Doubler

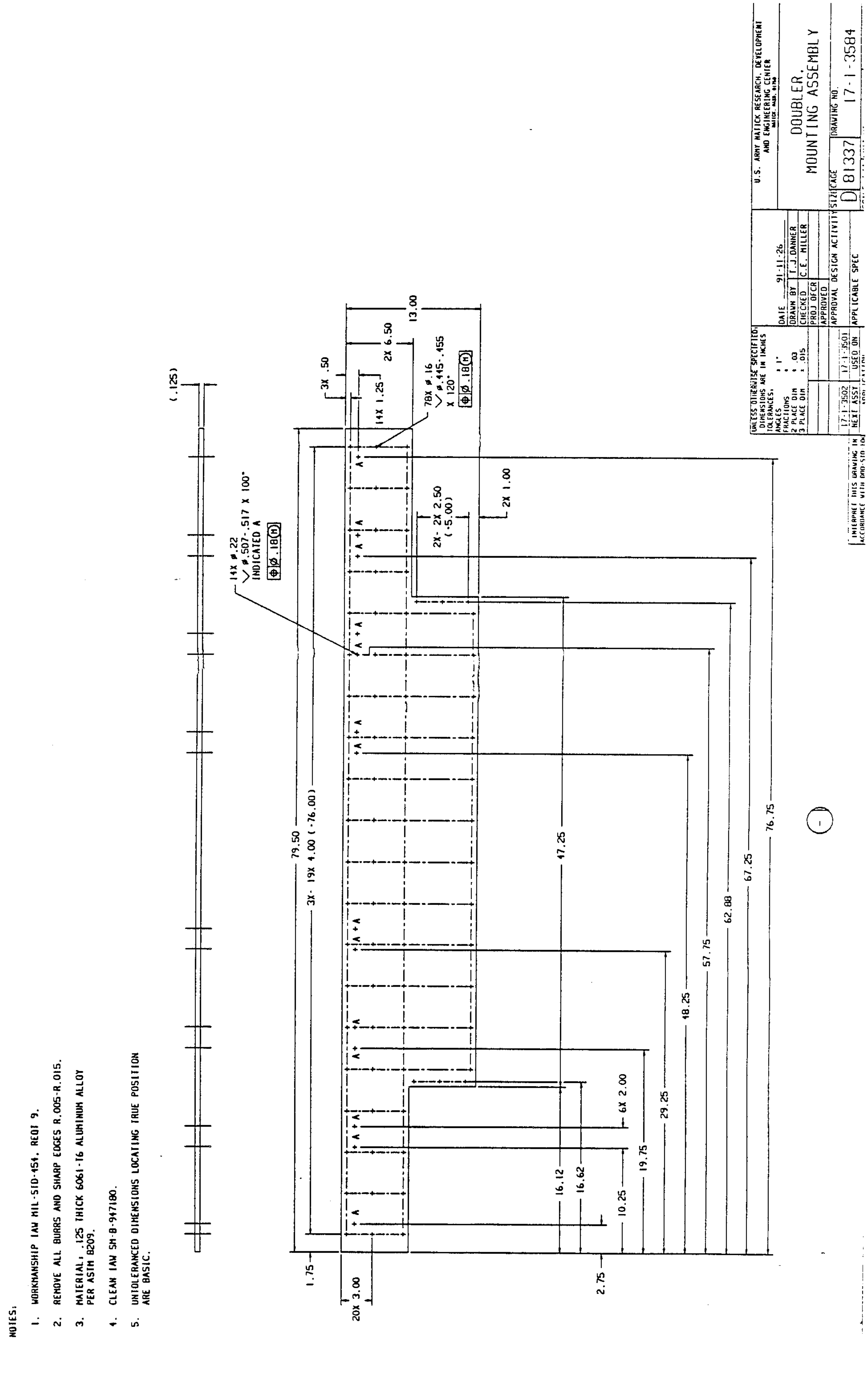

Fig. (5) Forward Doubler Plate

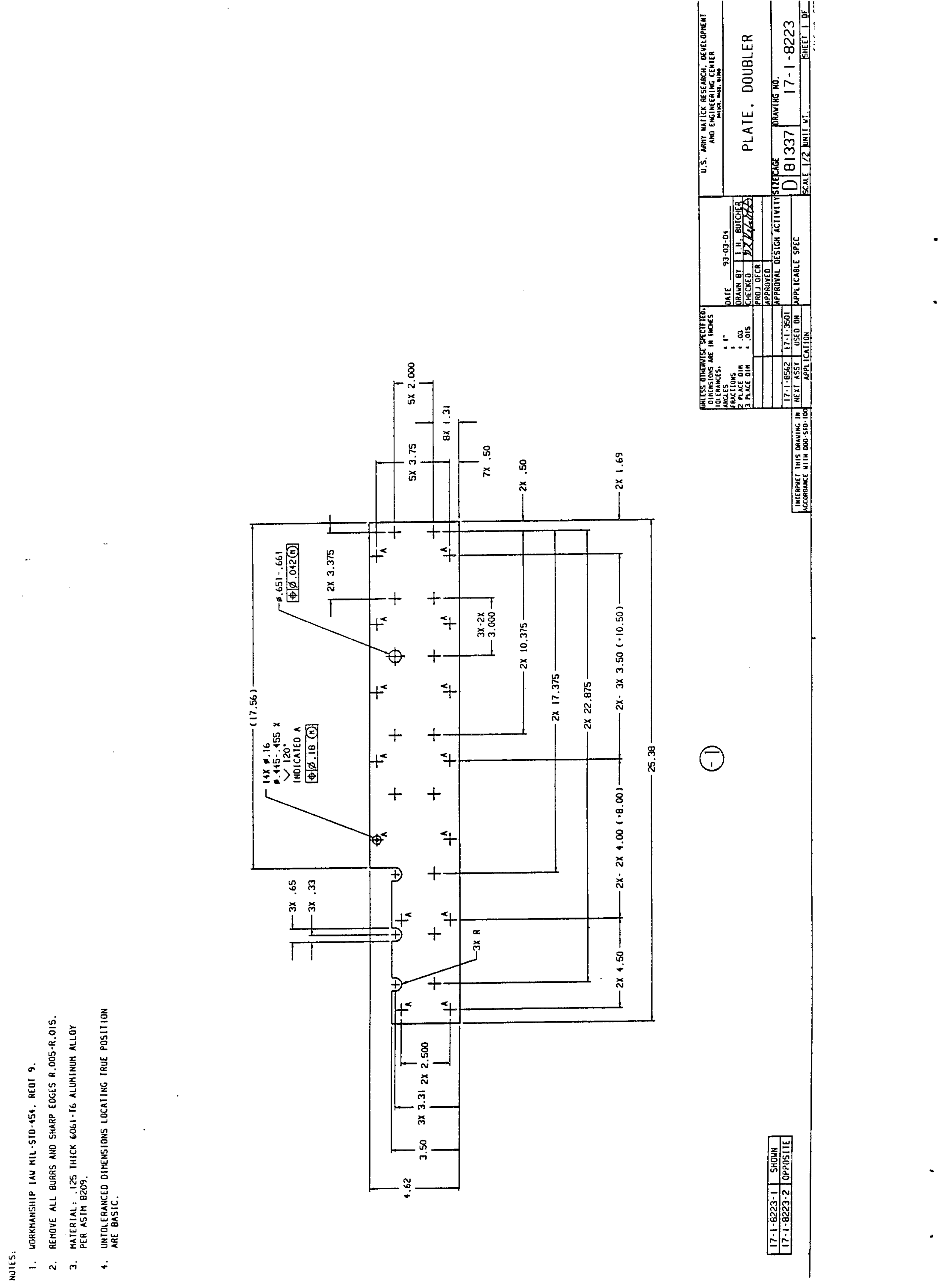

Fig. (6) Rear Doubler Plate Component #1

NOTES:

1. WORKMANSHIP IAW MIL-STD-454, REQT 9.
2. REMOVE ALL BURRS AND SHARP EDGES R.005-R.015.
3. MATERIAL: .125 THICK 6061-T6 ALUMINUM ALLOY PER ASTM B209.
4. CLEAN IAW SH-B-947180.
5. UNTOLERANCED DIMENSIONS LOCATING TRUE POSITION ARE BASIC.

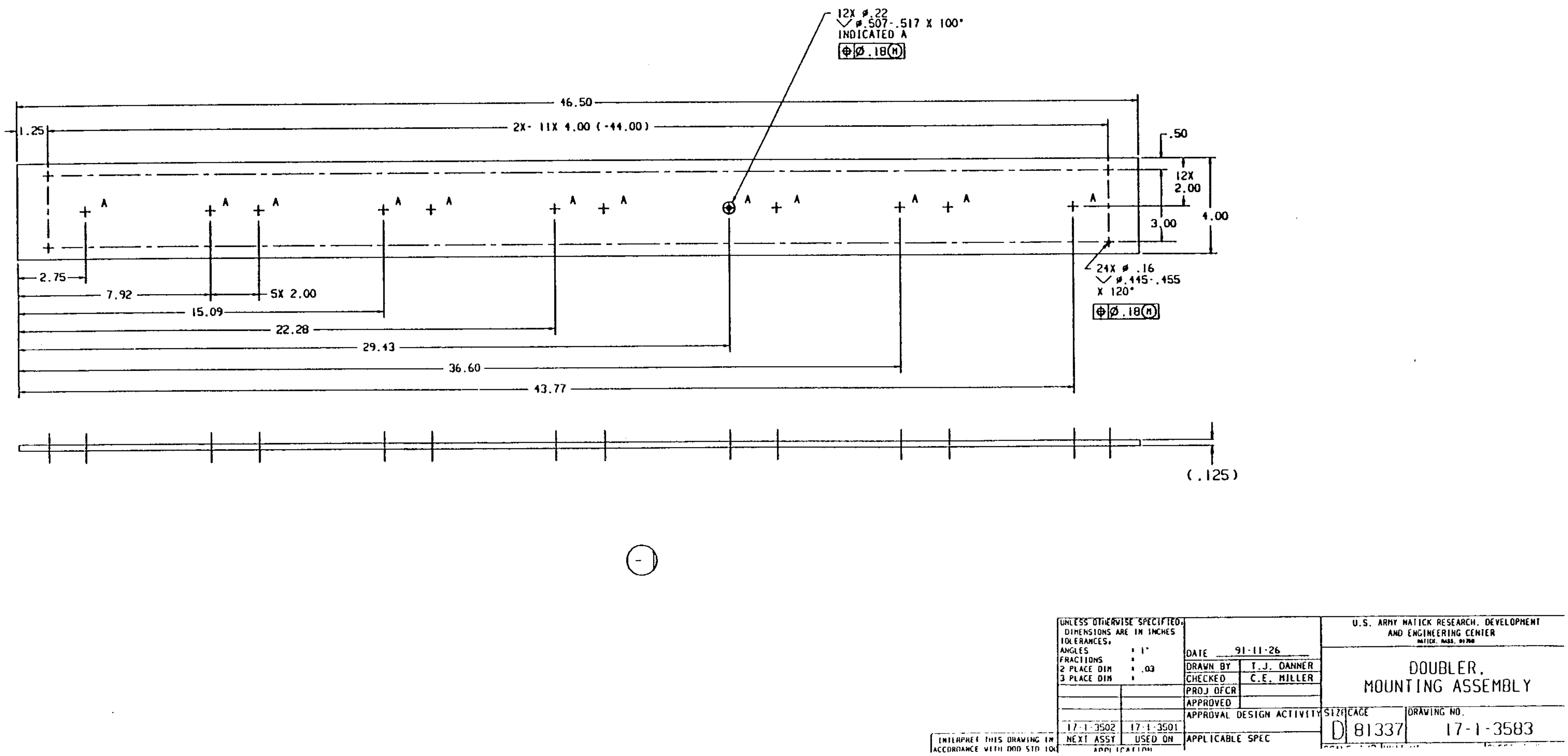

Fig. (7) Rear Doubler Plate Component #2

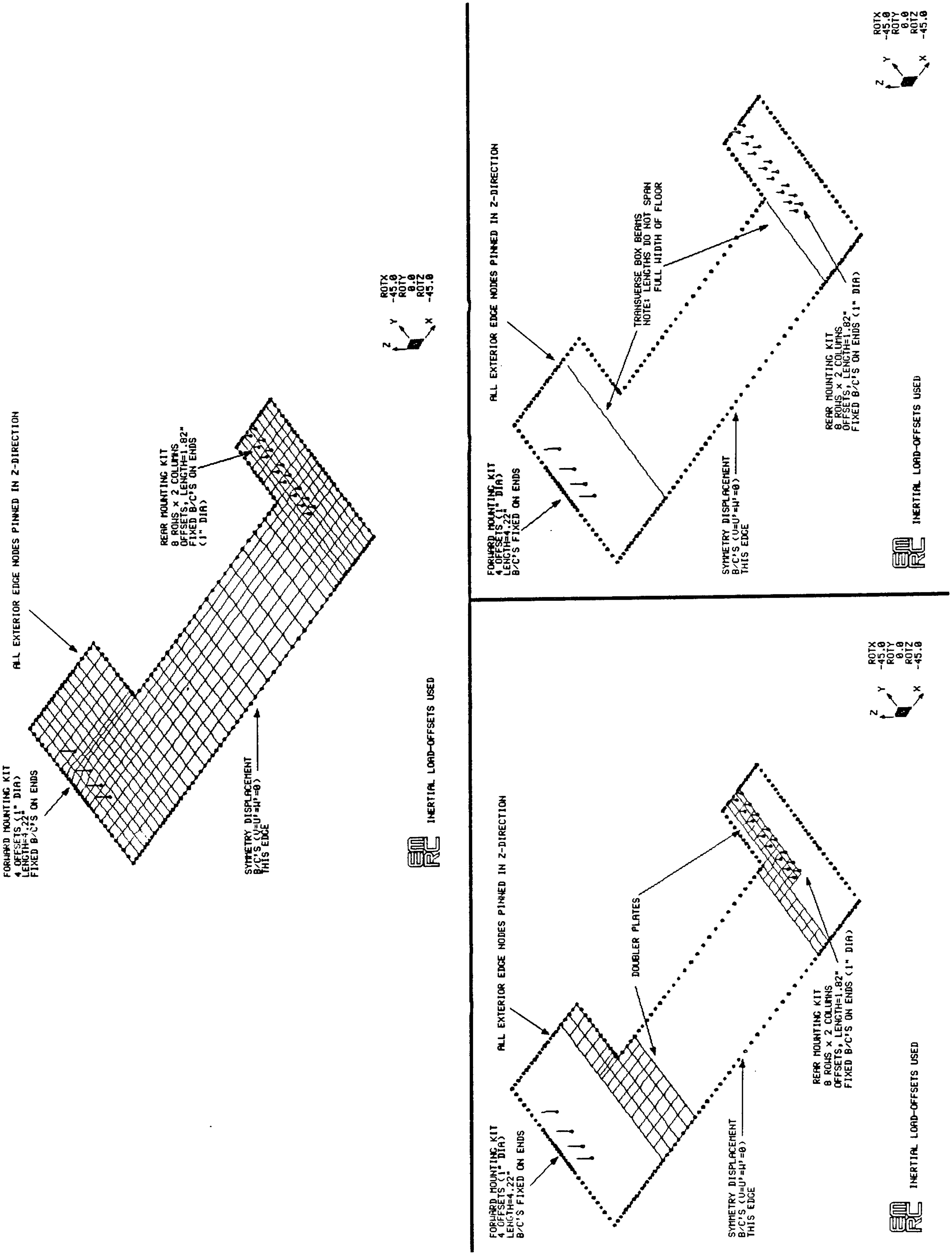

Fig. (8) Floor Panel Models w/ Reinforcements Shown

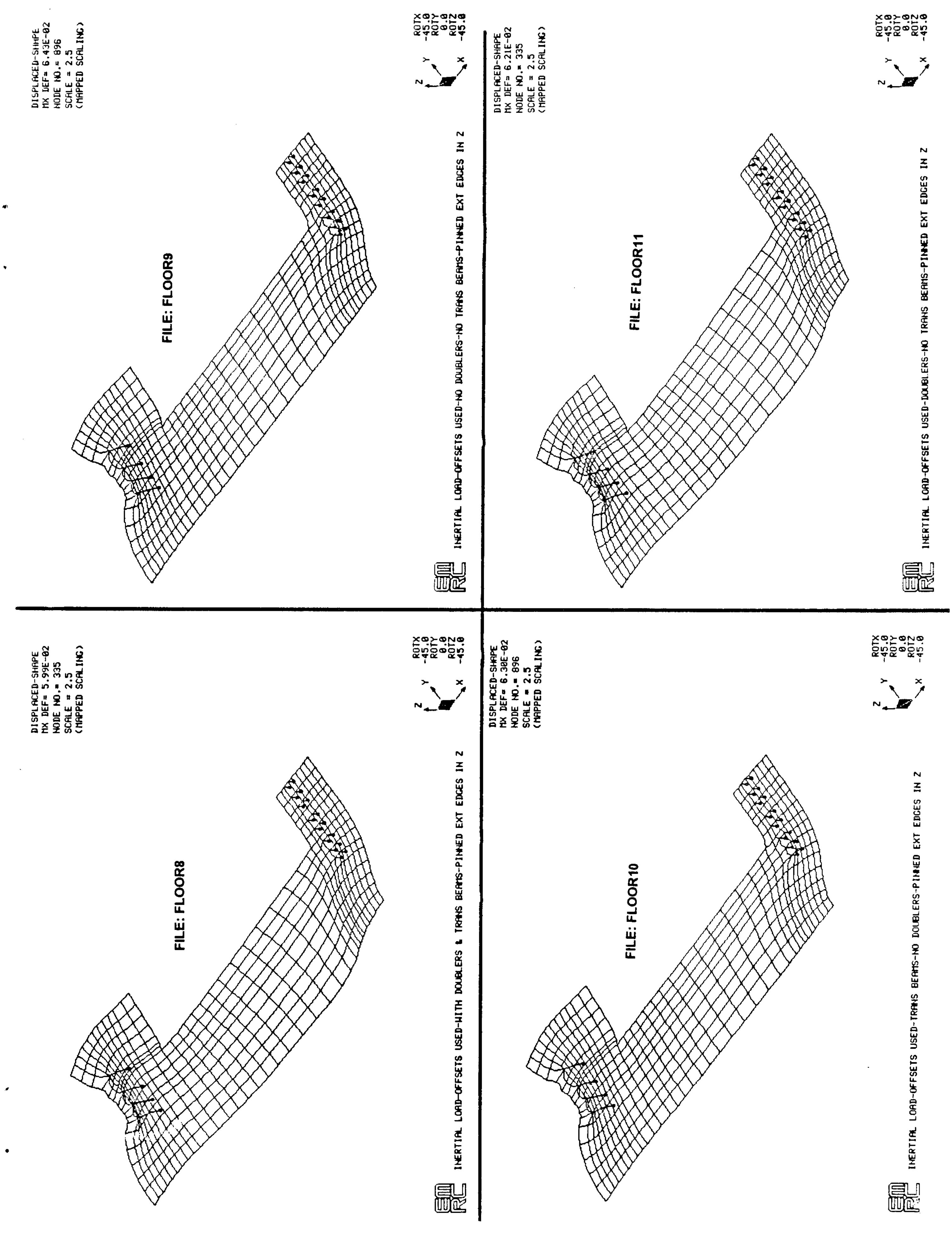

Fig. (9) Isometric Views of Displaced Floor Panel Models

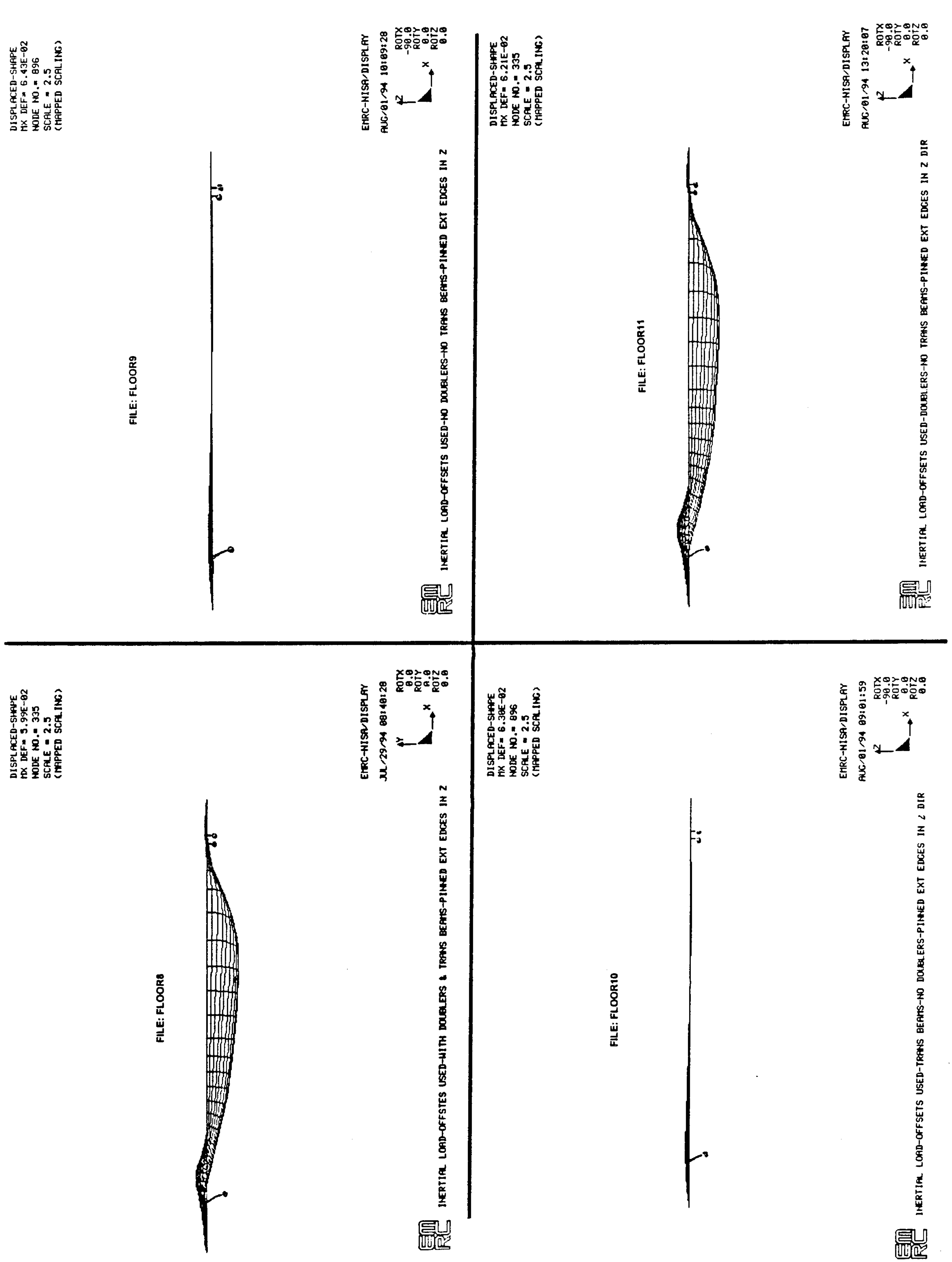

Fig. (10) Edge Views of Displaced Floor Panel Models

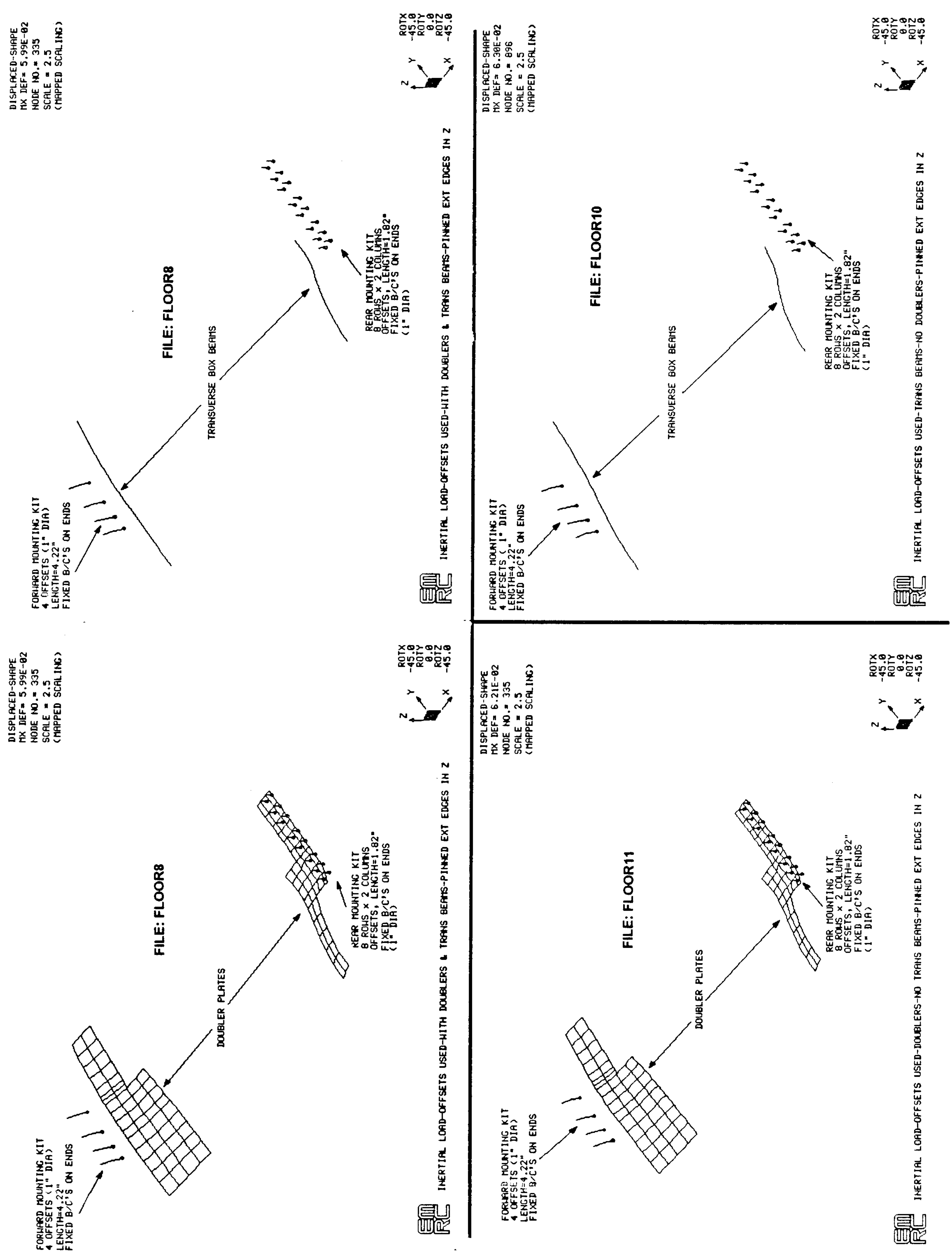

Fig. (11) Isometric Views of Displaced Doublers & Transverse Beams

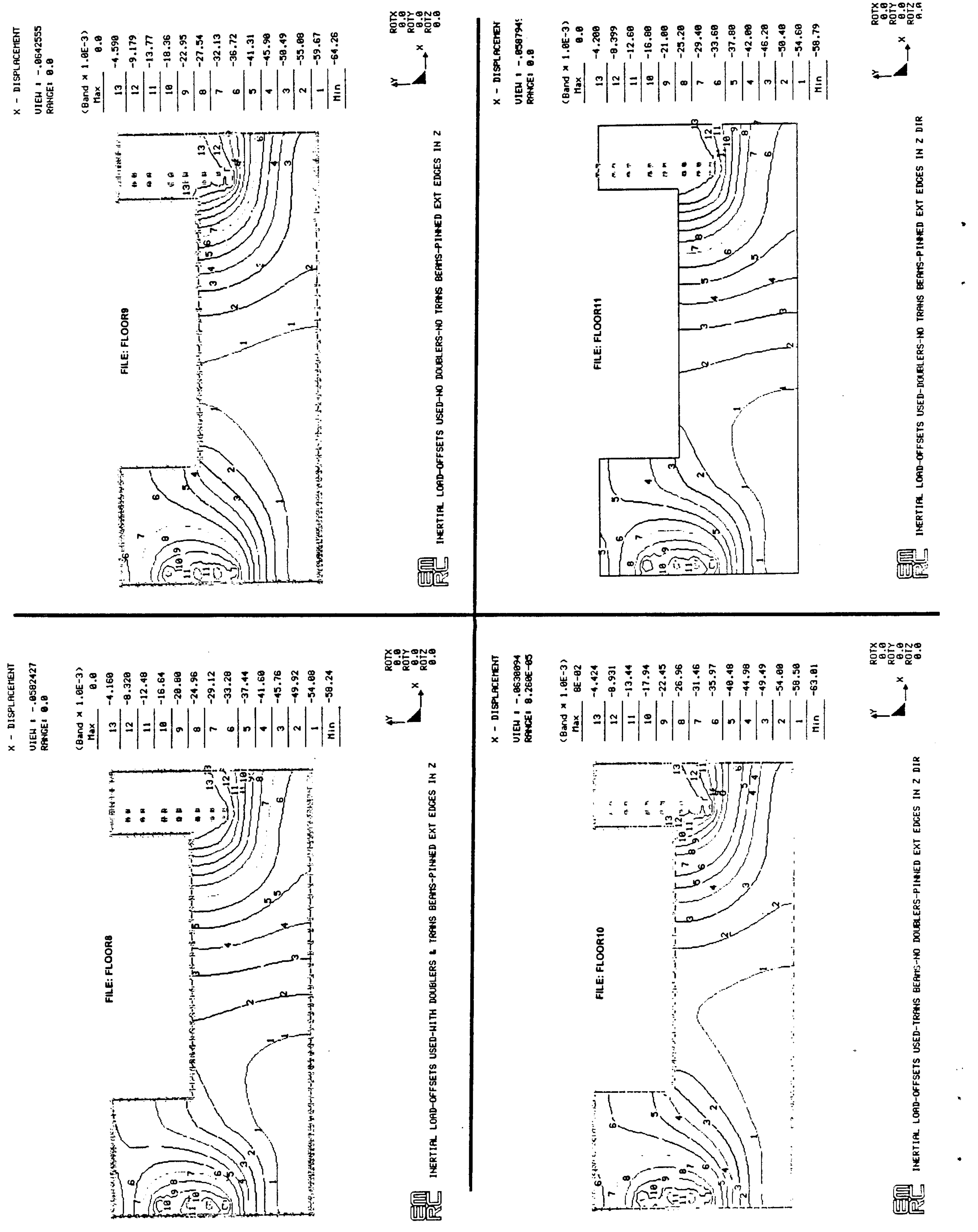

Fig. (12) X Displacement Component - Middle Surface

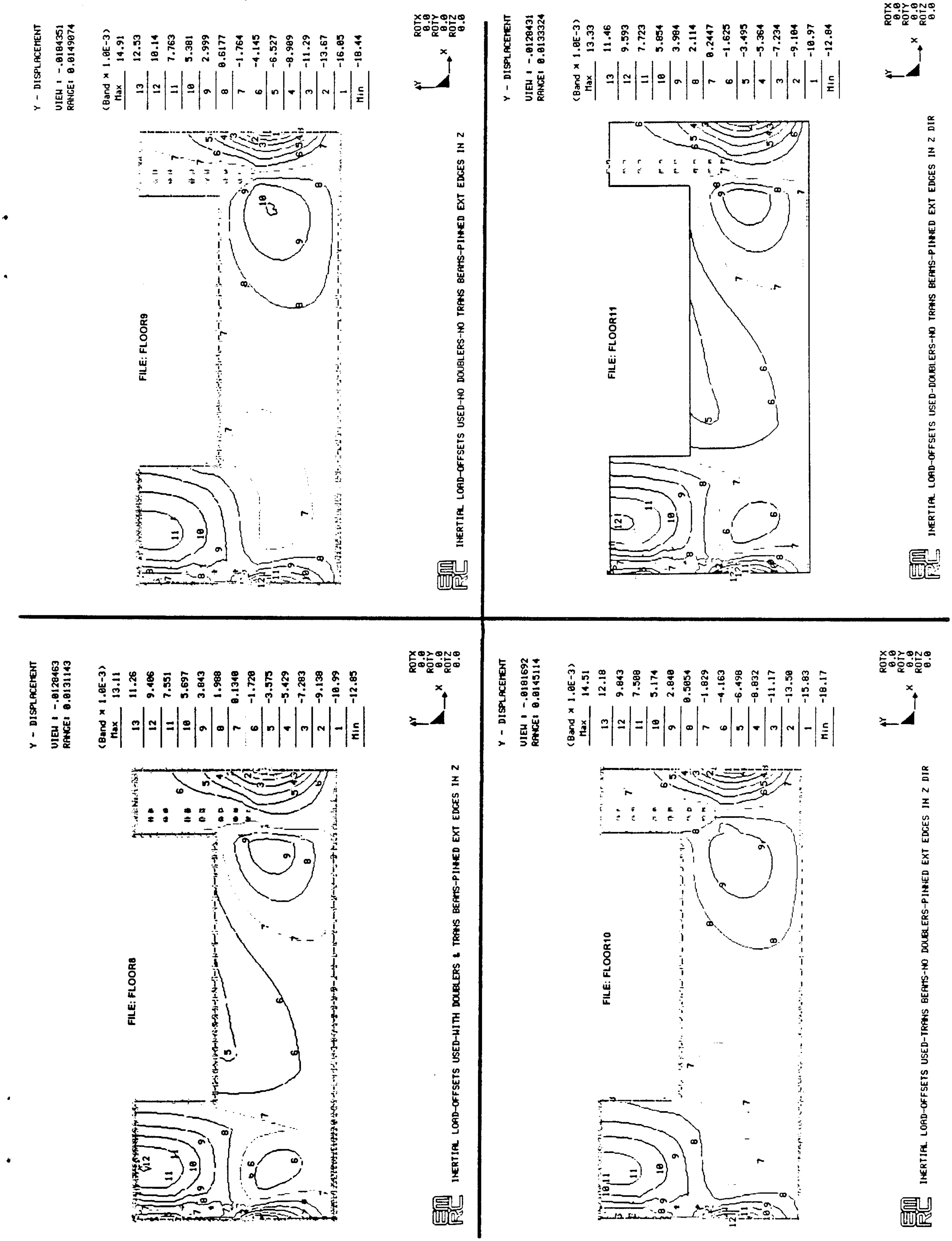

Fig. (13) Y Displacement Component - Middle Surface

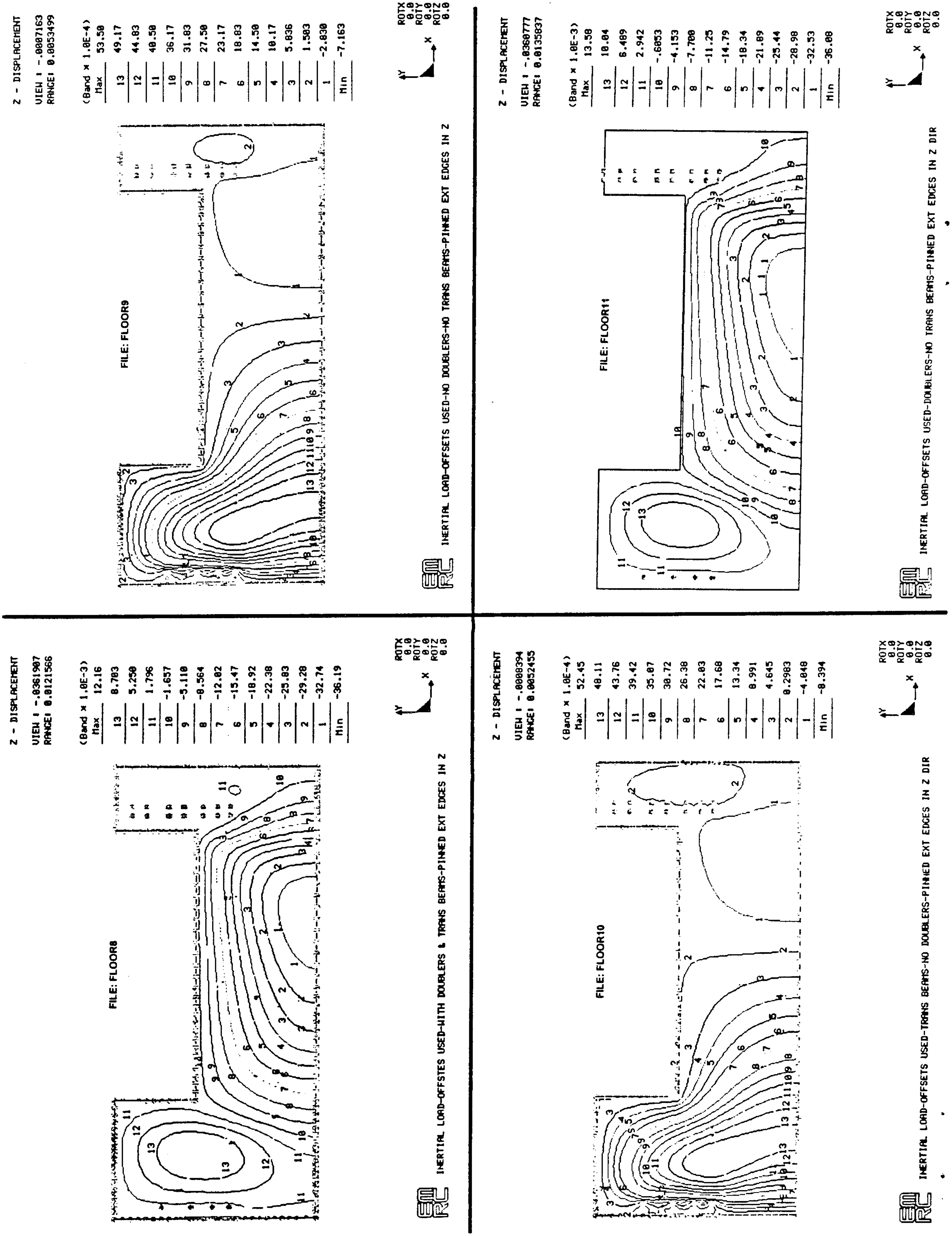

Fig. (14) Z Displacement Component - Middle Surface

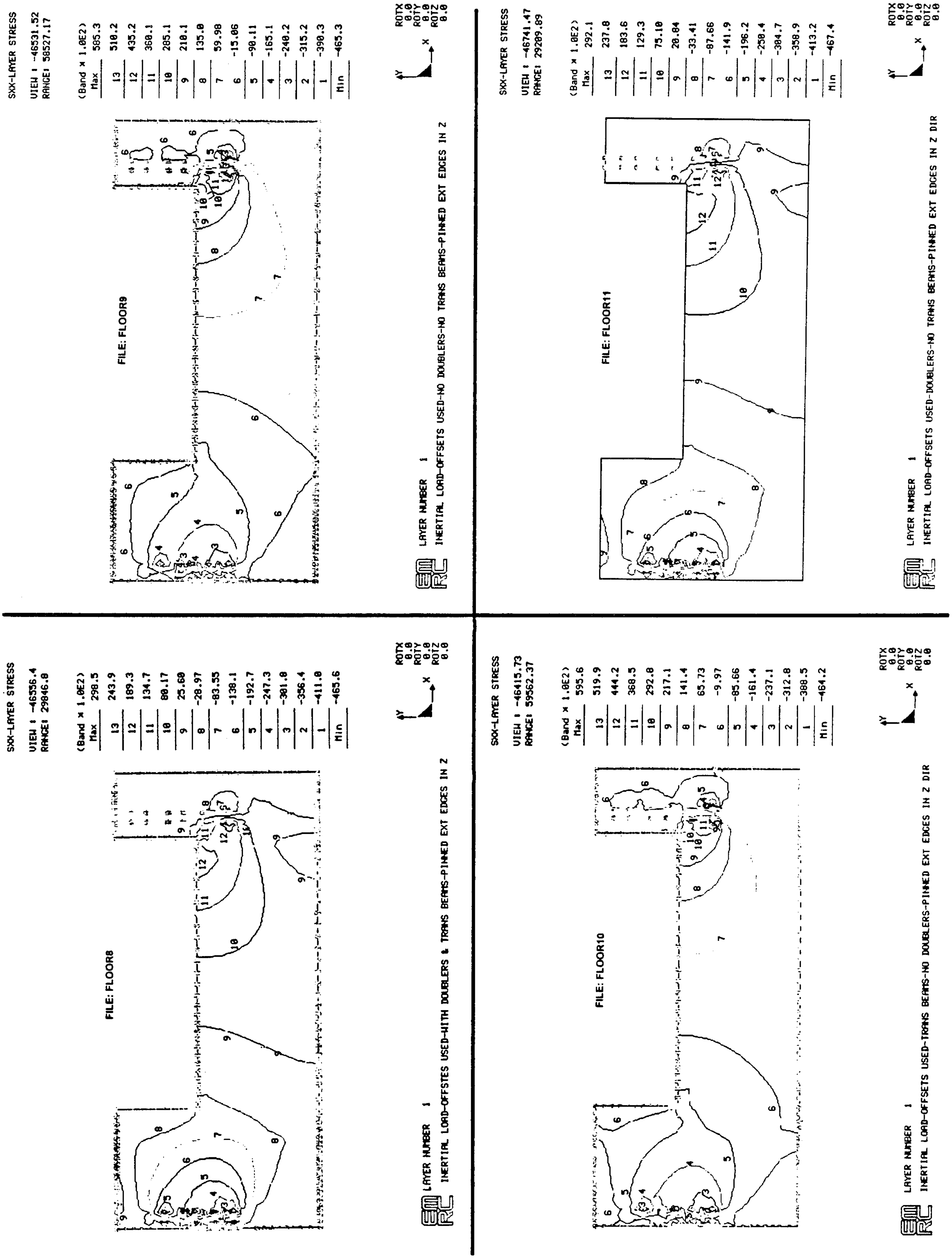

Fig. (15) Upper Face Sheet (Layer #1) - Sxx Stress Component

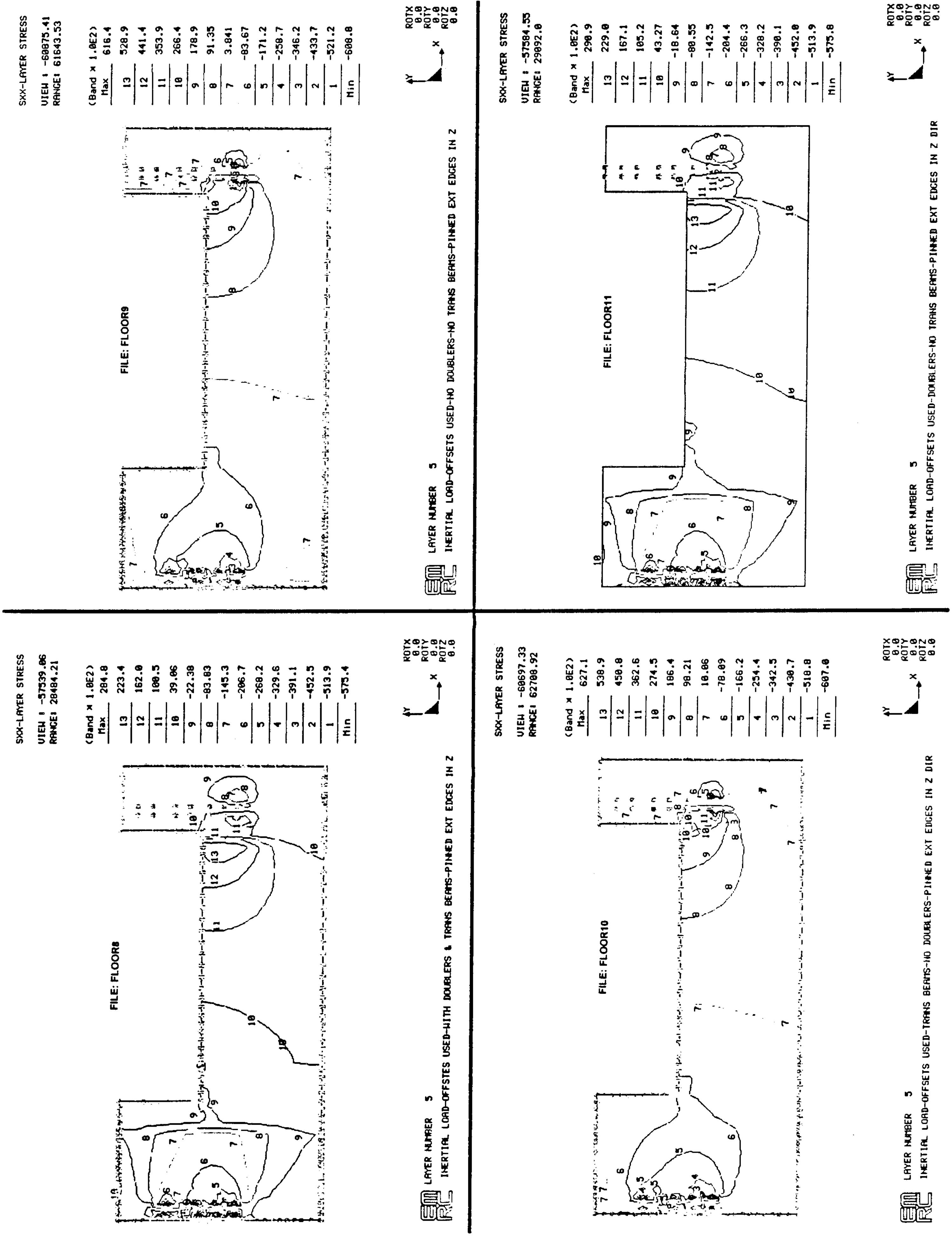

Fig. (16) Lower Face Sheet (Layer #5 Sxx Stress Component

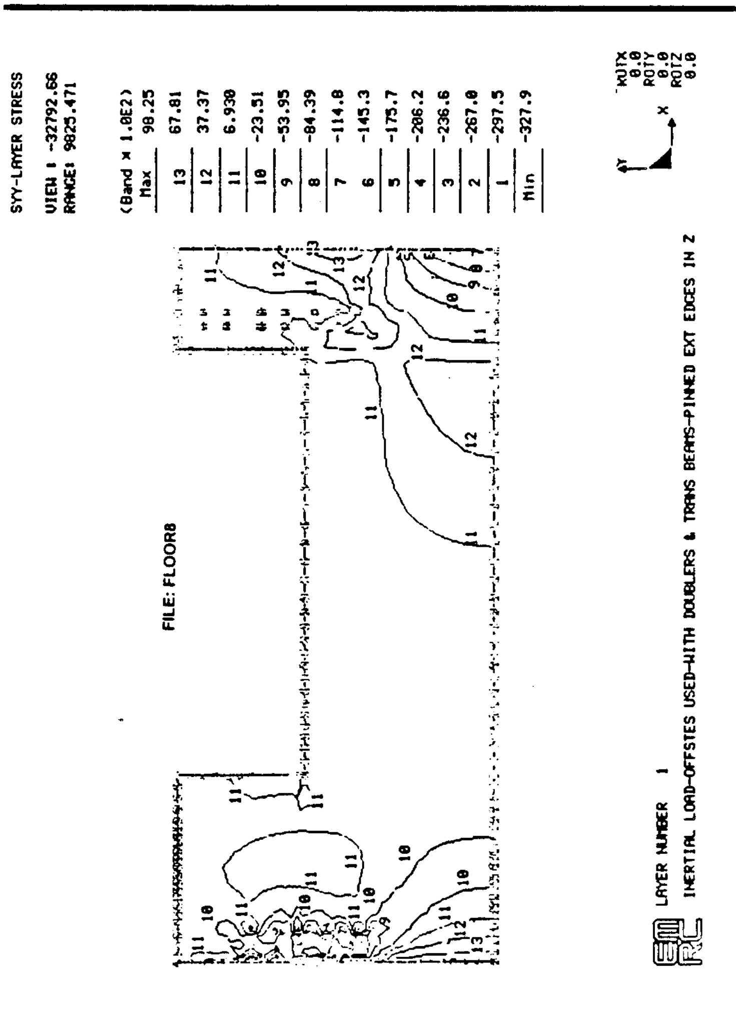

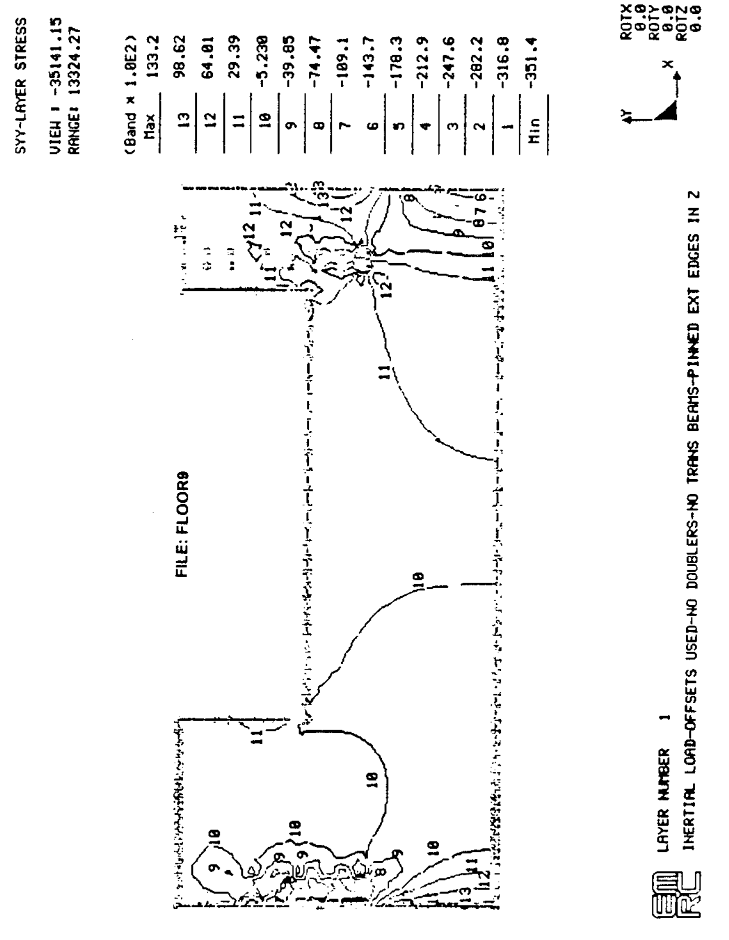

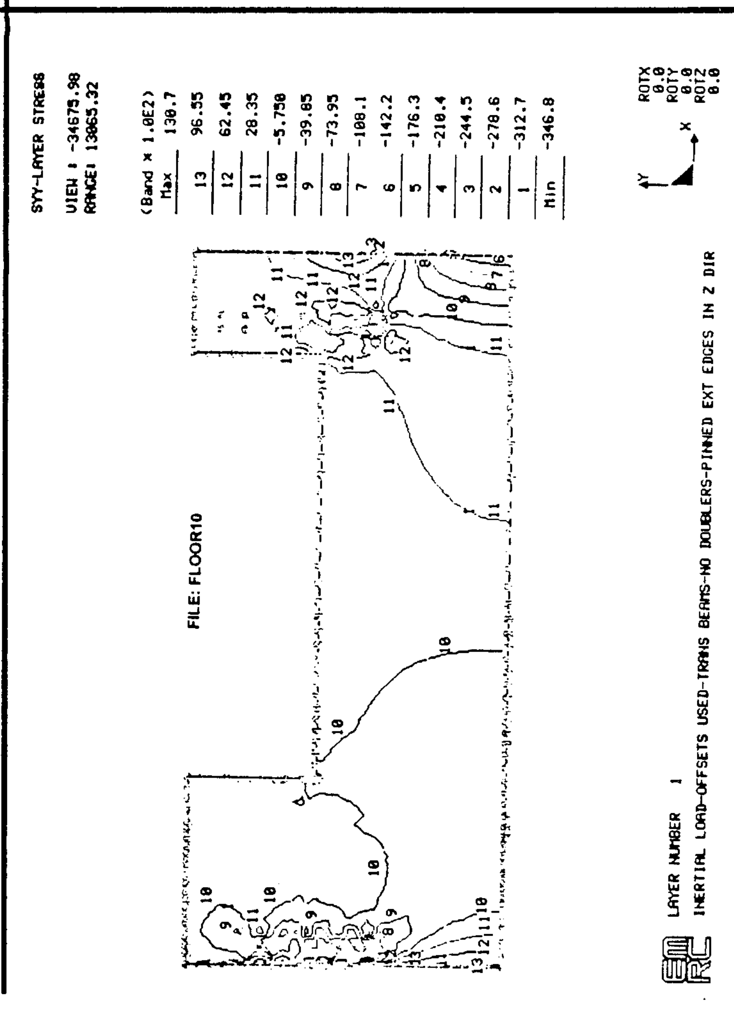

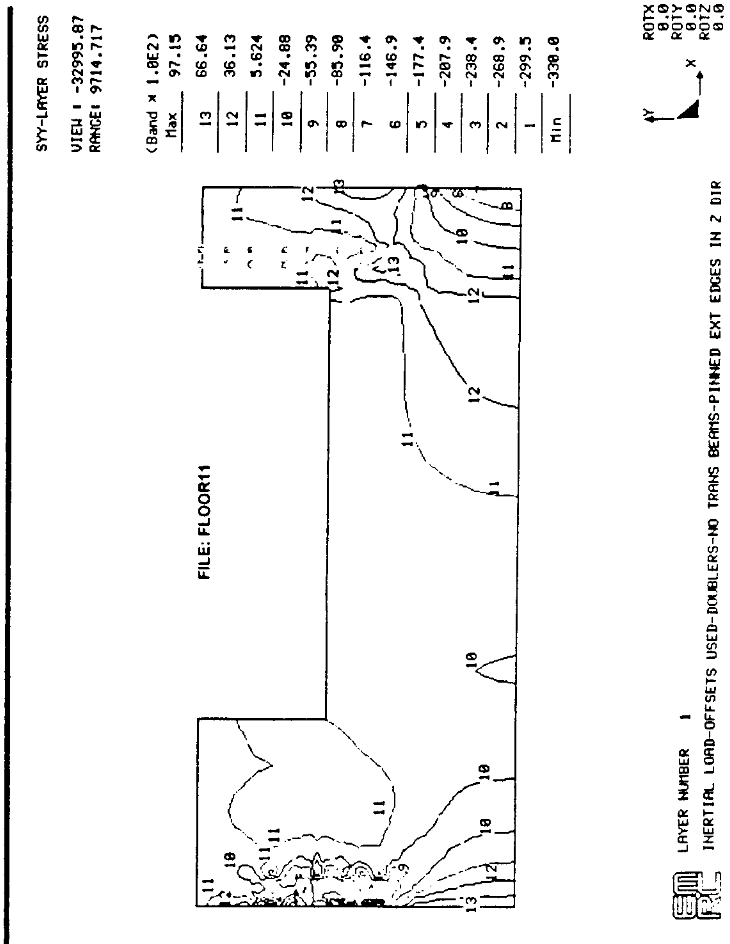

Fig. (17) Upper Face Sheet (Layer #1) - Syy Stress Component

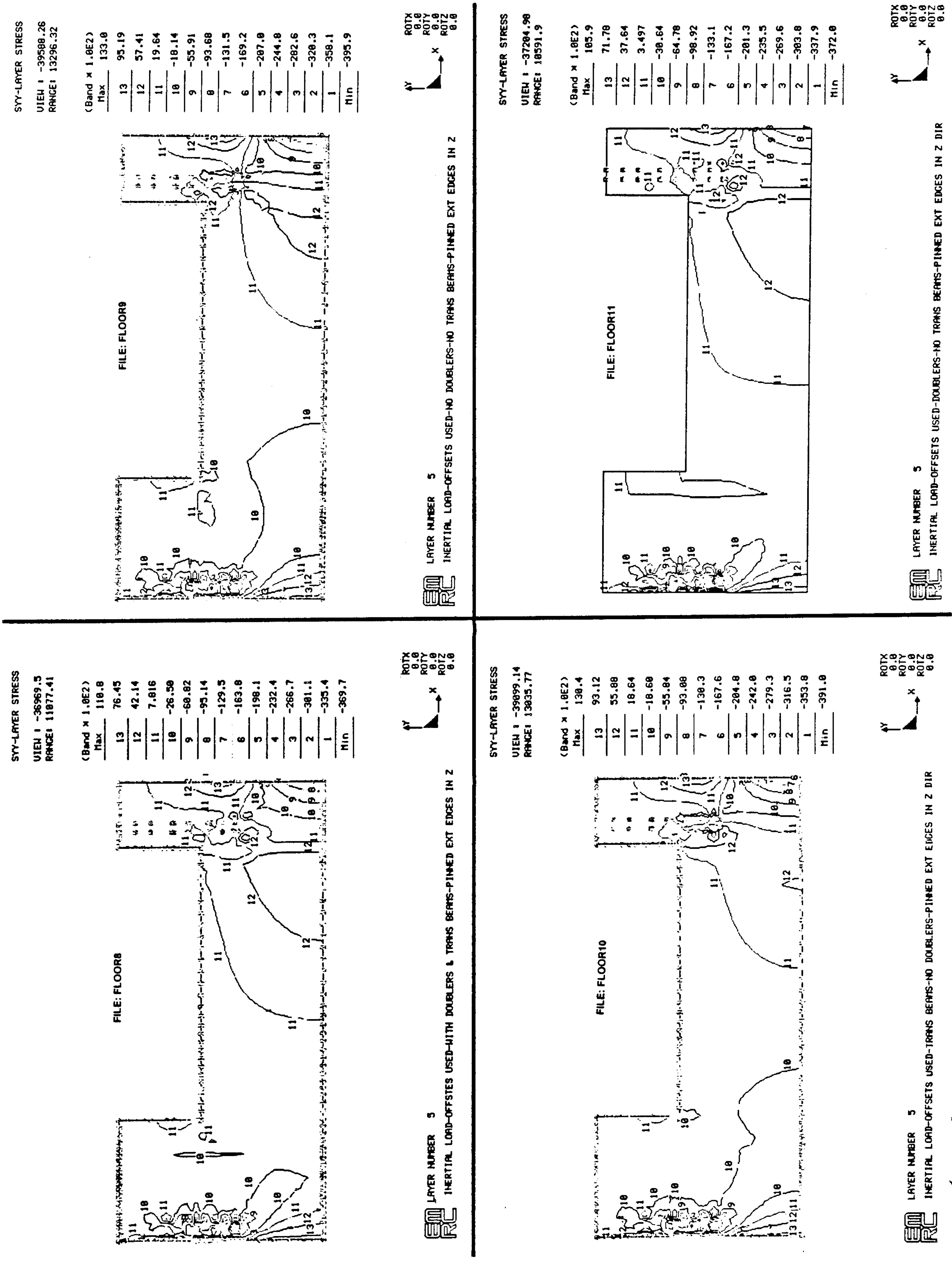

Fig. (18) Lower Face Sheet (Layer #5) - Syy Stress Component

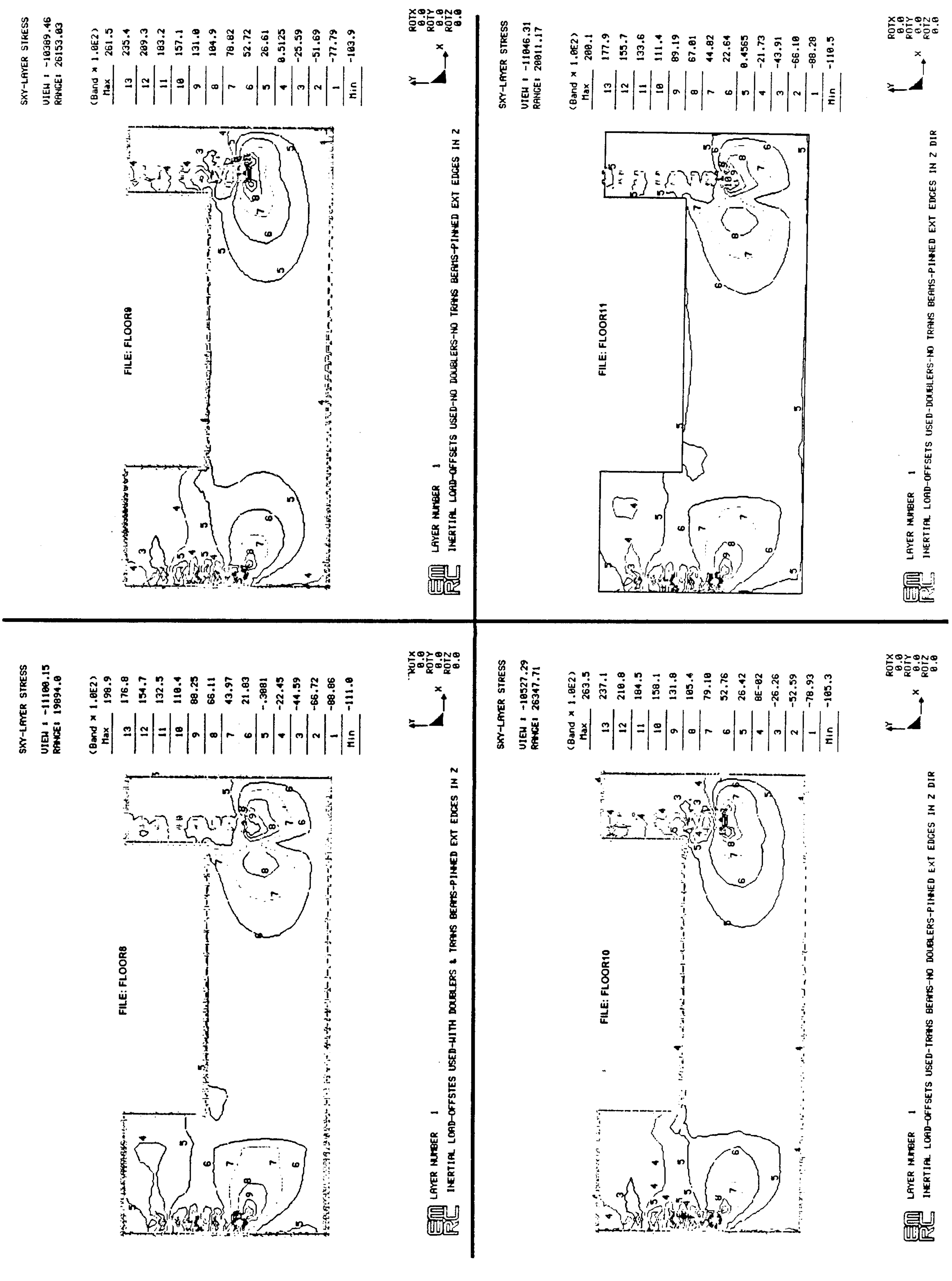

Fig. (19) Upper Face Sheet (Layer #1) - Sxy Stress Component

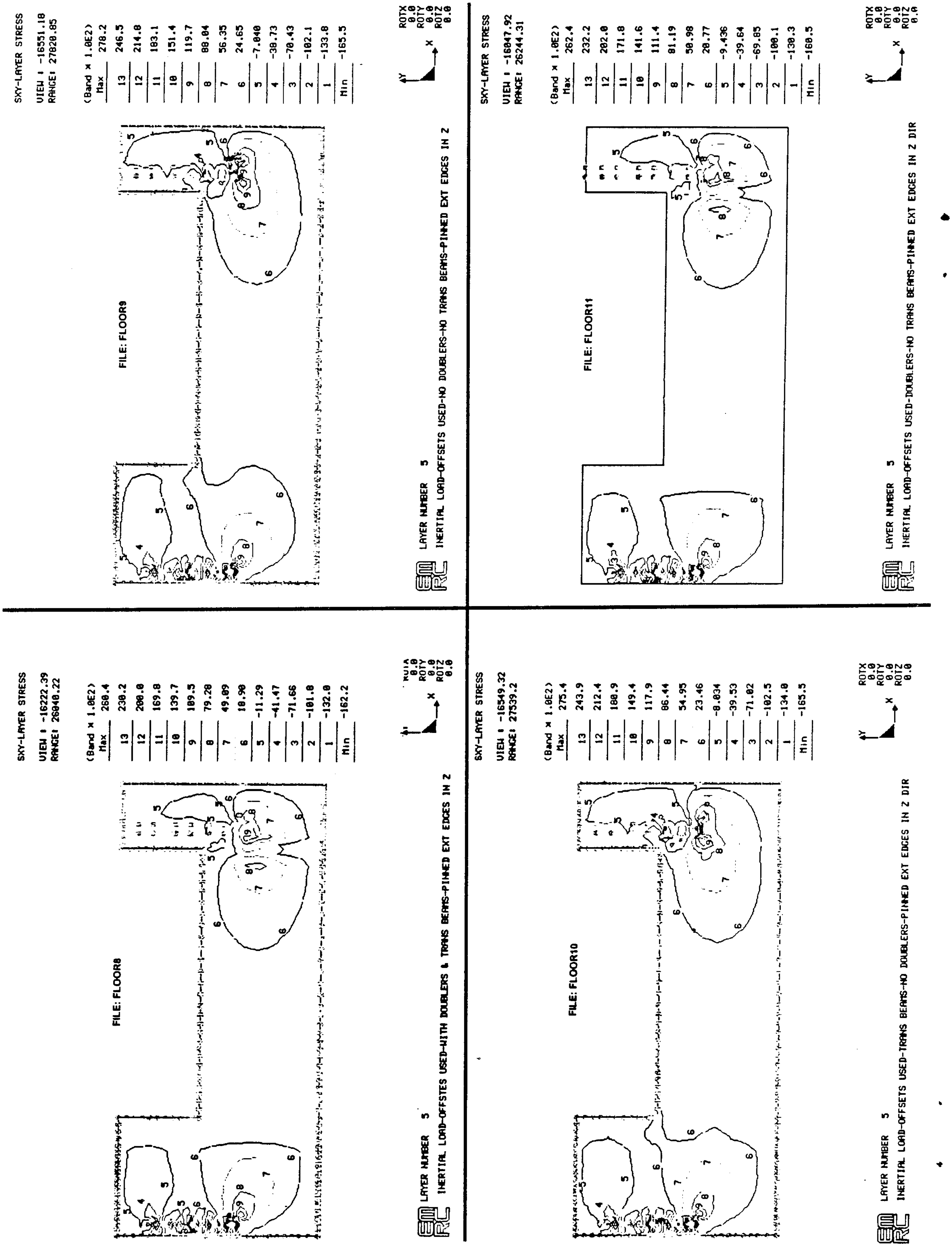

Fig. (20) Lower Face Sheet (Layer #5) - Sxy Stress Component

DISTRIBUTION LIST

No. of Copies	To
1	Office of the Under Secretary of Defense for Research and Engineering, The Pentagon, Washington, DC 20301
	Director, U.S. Army Research Laboratory, 2800 Powder Mill Road, Adelphi, MD 20783-1197
1	ATTN: AMSRL-OP-SD-TP, Technical Publishing Branch
1	AMSRL-OP-SD-TA, Records Management
1	AMSRL-OP-SD-TL, Technical Library
	Commander, Defense Technical Information Center, Cameron Station, Building 5, 5010 Duke Street, Alexandria, VA 23304-6145
2	ATTN: DTIC-FDAC
1	MIA/CINDAS, Purdue University, 2595 Yeager Road, West Lafayette, IN 47905
	Commander, Army Research Office, P.O. Box 12211, Research Triangle Park, NC 27709-2211
1	ATTN: Information Processing Office
	Commander, U.S. Army Materiel Command, 5001 Eisenhower Avenue, Alexandria, VA 22333
1	ATTN: AMCSCI
	Commander, U.S. Army Materiel Systems Analysis Activity, Aberdeen Proving Ground, MD 21005
1	ATTN: AMXSY-MP, H. Cohen
	Commander, U.S. Army Missile Command, Redstone Arsenal, AL 35809
1	ATTN: AMSMI-RD-CS-R/Doc
	Commander, U.S. Army Armament, Munitions and Chemical Command, Dover, NJ 07801
1	ATTN: Technical Library
	Commander, U.S. Army Natick Research, Development and Engineering Center Natick, MA 01760-5010
1	ATTN: SATNC-MI, Technical Library
	Commander, U.S. Army Satellite Communications Agency, Fort Monmouth, NJ 07703
1	ATTN: Technical Document Center
	Commander, U.S. Army Tank-Automotive Command, Warren, MI 48397-5000
1	ATTN: AMSTA-ZSK
1	AMSTA-TSL, Technical Library
	President, Airborne, Electronics and Special Warfare Board, Fort Bragg, NC 28307
1	ATTN: Library
	Director, U.S. Army Research Laboratory, Weapons Technology, Aberdeen Proving Ground, MD 21005-5066
1	ATTN: AMSRL-WT

No. of Copies	To
	Commander, Dugway Proving Ground, UT 84022
1	ATTN: Technical Library, Technical Information Division
	Commander, U.S. Army Research Laboratory, 2800 Powder Mill Road, Adelphi, MD 20783
1	ATTN: AMSRL-SS
	Director, Benet Weapons Laboratory, LCWSL, USA AMCCOM, Watervliet, NY 12189
1	ATTN: AMSMC-LCB-TL
1	AMSMC-LCB-R
1	AMSMC-LCB-RM
1	AMSMC-LCB-RP
	Commander, U.S. Army Foreign Science and Technology Center, 220 7th Street, N.E., Charlottesville, VA 22901-5396
3	ATTN: AIFRTC, Applied Technologies Branch, Gerald Schlesinger
	Commander, U.S. Army Aeromedical Research Unit, P.O. Box 577, Fort Rucker, AL 36360
1	ATTN: Technical Library
	U.S. Army Aviation Training Library, Fort Rucker, AL 36360
1	ATTN: Building 5906-5907
	Commander, U.S. Army Agency for Aviation Safety, Fort Rucker, AL 3636
1	ATTN: Technical Library
	Commander, Clarke Engineer School Library, 3202 Nebraska Ave., N., Fort Leonard Wood, MO 65473-5000
1	ATTN: Library
	Commander, U.S. Army Engineer Waterways Experiment Station, P.O. Box 631, Vicksburg, MS 39180
1	ATTN: Research Center Library
	Commandant, U.S. Army Quartermaster School, Fort Lee, VA 23801
1	ATTN: Quartermaster School Library
	Naval Research Laboratory, Washington, DC 20375
1	ATTN: Code 6384
	Chief of Naval Research, Arlington, VA 22217
1	ATTN: Code 471
	Commander, U.S. Air Force Wright Research and Development Center, Wright-Patterson Air Force Base, OH 45433-6523
1	ATTN: WRDC/MLLP, M. Forney, Jr.
1	WRDC/MLBC, Mr. Stanley Schulman
	U.S. Department of Commerce, National Institute of Standards and Technology, Gaithersburg, MD 20899
1	ATTN: Stephen M Hsu, Chief, Ceramics Division, Institute for Materials Science and Engineering

No. of Copies	To
1	Committee on Marine Structures, Marine Board, National Research Council, 2101 Constitution Avenue, N.W., Washington, DC 20418
1	Materials Sciences Corporation, Suite 250, 500 Office Center Drive, Fort Washington, PA 19034
1	Charles Stark Draper Laboratory, 555 Technology Square, Cambridge, MA 02139
	General Dynamics, Convair Aerospace Division, P.O. Box 748, Fort Worth, TX 76101
1	ATTN: Mfg. Engineering Technical Library
	Plastics Technical Evaluation Center, PLASTEC, ARDEC, Bldg. 355N, Picatinny Arsenal, NJ 07806-5000
1	ATTN: Harry Pebly
1	Department of the Army, Aerostructures Directorate, MS-266, U.S. Army Aviation R&T Activity - AVSCOM, Langley Research Center, Hampton, VA 23665-5225
1	NASA - Langley Research Center, Hampton, VA 23665-5255
	U.S. Army Vehicle Propulsion Directorate, NASA Lewis Research Center, 2100 Brookpark Road, Cleveland, OH 44135-3191
1	ATTN: AMSRL-VP
	Director, Defense Intelligence Agency, Washington, DC 20340-6053
1	ATTN: ODT-5A, Mr. Frank Jaeger
	U.S. Army Communications and Electronics Command, Fort Monmouth, NJ 07703
1	ATTN: Technical Library
	U.S. Army Research Laboratory, Electronic Power Sources Directorate, Fort Monmouth, NJ 07703
1	ATTN: Technical Library
	Director, U.S. Army Research Laboratory, Watertown, MA 02172-0001
2	ATTN: AMSRL-OP-WT-IS, Technical Library
5	Authors

DEPARTMENT OF THE ARMY
U.S. ARMY RESEARCH LABORATORY
ATTN: Visual Information Unit
AMSRL-OP-WT-IS
Watertown, Massachusetts 02172-0001